Kudchodkar *et al.*
Translational Medicine Communications (2022) 7:16
https://doi.org/10.1186/s41231-022-00121-9

Translational Medicine Communications

RESEARCH Open Access

Characterization of a small molecule modulator of inflammatory cytokine production

Sagar B Kudchodkar[1,2], Paolo Fagone[2,3], Omkar U Kawalekar[2], Moonsup Jeong[1], Christine C Roberts[1], Hyojin Lee[1], Youngran Cho[1], Areum Gil[1], Yeeun Oh[1], Bohyun Jeon[1], Gee Ho Park[1], Young K Park[1], Ferdinando Nicoletti[3], Joel N Maslow[1] and Kar Muthumani[1,2*]

Abstract

In the present study, the effect(s) of the immunomodulatory drug GLS-1027 on various cell types involved in inflammation were investigated. GLS-1027 reduced LPS-stimulated secretion of pro-inflammatory cytokines by macrophage or monocytic cells and cell lines. This reduction was likely due in part to decreased activation of NF-κB family transcription factors and inhibition of p38 MAPK signaling in GLS-1027-treated cells. Independent from its effects on macrophages, GLS-1027 inhibited dendritic cell maturation and differentiation of naïve $CD4^+$ T cells into Th17 cells, reducing the production of typical pro-inflammatory cytokines associated with both processes. In vivo administration of GLS-1027 prevented the development of type 1 diabetes in NOD mice which correlated with reduced serum levels of IL17A in GLS-1027 treated animals and reduced ex vivo production of IL17A from both spleen and lymph-node cells. Overall, our data show that GLS-1027 can reduce inflammation through multiple actions, including the reduction of pro-inflammatory cytokine production by innate immune cells, the inhibition of dendritic cells maturation, and the inhibition of Th17 cells polarization.

Keywords: GLS-1027, Pro-inflammatory cytokines, Inflammation, Th17 cells, Type 1 diabetes mellitus, NOD mice, Inflammatory disorders

Introduction

Inflammation is a complex biologic process initiated in response to stimuli that are, or are potentially, harmful to an organism [1–4]. These stimuli include invading pathogens, dying cells, chemicals, and exposure to extreme temperatures [3]. The innate immune system senses these irritants and initiates a non-specific inflammatory response to deal with the actual or potential threat. An acute inflammatory response can usually eliminate the source of damage and thus be considered beneficial. However, dysregulation of the inflammatory response could lead to diseases characterized by excessive damage to healthy tissues or lead to chronic inflammation [3].

Inflammation is initiated by stimuli such as pathogen-associated molecular patterns (PAMPs) from invading pathogens or from damage-associated molecular patterns (DAMPs) that are produced by stressed or dying cells [4]. The PAMPs and DAMPs are sensed by pattern recognition receptors (PRRs) such as Toll-like receptors (TLRs), found on the surface of innate immune cells, as well as NOD-like receptors (NLRs) and RIG-I-like receptors (RLRs), found in the cytoplasm of innate immune cells [5–7]. Innate immune cells bearing PRRs, including macrophages, monocytes, and dendritic cells, secrete various chemokines and cytokines upon PRR stimulation that promote recruitment of immune cells to the site of inflammation and the activation of effector mechanisms [8, 9]. Initiation of inflammation also activates the complement system, causes mast cells to release histamine, and promotes prostaglandin production which

*Correspondence: kmuthumani@genels.us

[1] GeneOne Life Science Inc, Yeongdeungpo Gu, Seoul 07335, Korea
Full list of author information is available at the end of the article

contributes to vasodilation, increased blood flow, and increased vascular permeability that allows immune cells to enter the tissue where the inflammatory signal was generated [10]. Antigen presenting cells (APCs), such as dendritic cells, scavenge proteins released by the inflammatory response and take these to lymph nodes where they can stimulate naïve T cells and B cells [6, 11]. Naïve helper T (Th) cells can differentiate into one of several subsets that each secrete a unique panel of cytokines to engage different effector mechanisms tailored towards eliminating the specific nature of the threat [7]. Of these subtypes, Th17 cells, which play an important role in extracellular pathogen defense, have been found to possess a strong ability to cause inflammation and have been implicated in the pathology of autoimmune disease and inflammation [12]. As the pathogens and/or damaged cells that initiated the inflammatory response are removed, macrophages can switch to an anti-inflammatory (M2) phenotype and promote the depletion of cytotoxic mediators in part through producing anti-inflammatory cytokines such as IL-10 and TGF-β[6].

The immunomodulatory compound (S,R)-3-Phenyl-4,5-dihydro-5-isoxasole acetic acid (GLS-1027; formerly VGX-1027 or GIT27) blocks signaling downstream of toll like receptors 4, 2, and 6, can modulate expression of genes involved in antigen processing and presentation, and regulate immune activation [13, 14]. Treatment with GLS-1027 reduces inflammatory cytokines production in vitro and in vivo which has correlated with amelioration of disease in various animal models of immunoinflammatory and autoimmune diseases including rheumatoid arthritis [14] systemic lupus erythematosus [13] inflammatory bowel diseases [15], pleurisy [14] and inflammatory uveitis [16]. GLS-1027 treatment powerfully ameliorated clinical, histological and immunopathogenic signs of immunoinflammatory diabetes induced in CBA/H mice by multiple low doses of streptozotocin [17], and it inhibited expression of proinflammatory cytokines in the kidneys and adipose tissue, and improved extracellular matrix expansion and tubule interstitial fibrosis in obesity-related kidney disease [18, 19]. In rodent models of endotoxin-induced uveitis and acute inflammatory colitis GLS-1027 treatment ameliorated clinical signs of disease and reduced levels of inflammatory cytokines including IL-1β, TNF-α, IL-12p70, and IFN-γ [15, 16]. Other studies have found that GLS-1027 prevents airway inflammation and bronchial hyperresponsiveness induced by fine particulate matter ($PM_{2.5}$) [20] or LPS-induced acute lung injury (ALI) [21]. More recently and of particular relevance for the translation to the clinical setting, it has been shown that the nephrotoxic effects observed in patients with multiple myeloma due to the exuberant production of free light chains (FLCs) that overwhelm the endocytic capacity of proximal tubule cells occurs through a STAT1/HMGB1/TLR axis in a manner that is counteracted in vitro by GLS-1027 [22]. All these convergent and independent data on unique and pleiotropic immunomodulatory actions of GLS-1027 along with its completion of Phase I study [23] make this compound of highly relevant interest for use in different immunoinflammatory and autoimmune diseases and propelled this present study where we aimed to gain additional information on its mode of action both in vitro and in the NOD mouse that represents a well-known model of human type 1 diabetes.

In this study, we interrogate the effects of GLS-1027 on various immune cell types that mediate inflammation. We confirm that GLS-1027 inhibits cytokine production from macrophage and monocyte cells after stimulation with the TLR4 agonist, LPS. Treatment of macrophages with GLS-1027 inhibited activation of p38 MAPK signaling and NF-κB family transcription factors, downstream of TLR4 stimulation. Independent of its effects on macrophages/monocytes, GLS-1027 also impeded DCs maturation and development of inflammatory Th17 cells. Finally, we investigated the in vivo effect of GLS-1027 in a spontaneous model of type 1 diabetes, the NOD mouse. Administration of GLS-1027 was associated with a significant reduction in the incidence of overt diabetes which correlated with reduced serum levels of IL17A in vivo and decreased production of IL17A by cells of GLS-1027 treated mice stimulated ex vivo. Together these studies show that GLS-1027 modulates inflammation by affecting signaling downstream of PRRs and cytokine receptors to prevent activation of transcription factors that mediate pro-inflammatory cytokine production, maturation of dendritic cells and differentiation of Th17 cells. Overall, these studies support further studies of GLS-1027 for the treatment of autoimmune and other inflammatory diseases.

Materials and methods

Reagents

Recombinant human IL-1β, IL-4, TNF-α, GM-CSF and anti-CD3 mAbs, and fluorophore-conjugated, human mAbs to cell-specific surface proteins CD3, CD4, CD8, CD14, CD40, CD83, CD86 and HLA-DR and their matched isotypes were purchased from BD Biosciences (San Diego, CA, USA). PHA, LPS (*E. coli* 026:56) was purchased from Sigma-Aldrich (Saint Louis, MO, USA). Phosflow Lyse/Fix buffer, Phosflow Perm/Wash Buffer I and Stain Buffer were purchased from BD Pharmingen (San Diego, CA, USA).

Preparation of peripheral blood mononuclear cells (PBMCs) and CD4$^+$T Cells.

Human PBMC's and T cells were procured through the University of Pennsylvania Human Immunology Core. Cells were obtained from healthy donors by leukapheresis and were separated into subsets by negative selection using the Rosette-Sep platform developed by STEMCELL Technologies. CD4$^+$ T cells were enriched from PBMC's using negative selection by using antibodies targeting cell surface proteins on human hematopoietic cells (CD16$^+$, CD19$^+$, CD36$^+$ and CD56$^+$) and glycophorin A on RBCs. The collected cells were washed three times with PBS and were subsequently grown in RPMI-1640 medium (Invitrogen, CA, USA) supplemented with 10% heat-inactivated fetal calf serum (Invitrogen, CA, USA), 100U/ penicillin and 100 µγ/ streptomycin (Invitrogen, CA, USA). Cells were cultured at 37°C in a humidified 5% CO_2 atmosphere [24].

Generation and maturation of DCs

Human monocytes were purchased from the Human Immunology Core, University of Pennsylvania School of Medicine. Monocytes (1×10^6) were cultured in 6-well flat bottom plates supplemented with 1000U/ recombinant human granulocyte–macrophage colony-stimulating factor (GM-CSF; Cat #: 215-GM) and 1000U/ human recombinant IL-4 (Cat#:204-IL) from R&D Systems, MN, USA for the generation of immature DC's. Day 6 immature DC's were matured as described with modification [25]. For differentiation into mature DC's (mDC's), immature DC (imDC's) were additionally stimulated on day 4 with 10 ng/ml rTNF-α or 10 µγ/ml LPS. Immature DC typically were HLA-DR^{++}, CD86^{++}, CD83$^{-/weak}$ and CD14^{weak}, whereas mature DC were HLA-DR^{+++}, CD86^{++++}, CD83^{+++} and CD14$^-$. After 6 days of culture, the cells were harvested, pooled together, and the cells were fixed using a BD Cytofix/Cytoperm™ Plus kit (Cat #: 555,028; BD Biosciences) as per manufacturer's protocol, and stained with fluorochrome-conjugated monoclonal antibodies (mAbs) specific for cell surface antigens. Culture supernatants were collected at various time points and kept frozen at -80 °C for assay of cytokine concentrations. All cytokines used in this study were recombinant human proteins and were used at plateau concentration to induce the optimal generation of DC's as previously reported [26].

In vitro differentiation and expansion of Th17 cells

Naïve CD4$^+$T cells (5×10^5) were cultured in complete medium containing 10% FBS and 300 units/ml human IL-2 in 48-well plates and stimulated with plate-bound anti-CD3 (4 µg). Cells were differentiated towards the Th17 lineage by culturing them with 10 ng/ml TGF-β, 10 ng/ml IL-1β, 25 ng/ml IL-6 and 10 ng/ml IL-23 (R&D Systems) for 6 days. For intracellular staining, cells were restimulated with 50 ng/ml PMA (Sigma) and 1 µg/ml ionomycin (Life Technologies) and treated with Golgi-Blocker (BD Biosciences) for 4 h., after which IL-17 and IFN-γ-producing cells were analyzed with intracellular staining. For the Th17 cells assay, six days after culture, CD4$^+$ cells were washed with PBS and stimulated with phorbol 12-myristate 13-acetate (PMA) and ionomycin. After incubated with protein transport inhibitor (BD PharMingen, CA, USA) to prevent cytokine secretion, the cells were stained with anti-CD4-FITC (BD PharMingen, CA, USA), treated with cytofix/cytoperm (BD PharMingen), and the stained with anti-IL-17A-PE (eBioscience, CA, USA) and anti- IFN-γ-PECy7 (BD PharMingen, CA, USA) antibodies. After washes, the cells were analyzed on a flow cytometer.

Preparation of GLS-1027 and treatment, MTT viability cytokine analysis, flow cytometry analysis

GLS-1027 was prepared in Na_2HPO_4 buffer as described previously [17]. Human PBMCs were resuspended to a concentration of 5×10^6 cells/ml in RPMI1640 media and were treated with 5 µγ/ml of LPS and 100 µM, 10 µM, 1 µM, 0.1 µM or 0.01 µM of GLS-1027 drug was then added to the wells. Culture supernatants were collected at 24, 48, 72 and 96 h. intervals and stored at -20 °C until all samples collected for analysis [27].

The quantities of TNF-α and IL-1β in the culture supernatants were determined by a sandwich ELISA using mAbs specific for each cytokine, as previously described in 96-well microtiter plates (R&D Systems, MN, USA) [28]. Results are expressed as the means of duplicate assays. The level of IL-23 in supernatants was measured using the human IL-23 ELISA kit (eBioscience, CA, USA). This sandwich ELISA employs a specific capture antibody and a p40-specific detection antibody rendering detection of the IL-23 heterodimer. Avidin-HRP conjugate was added at 1/250 dilution, followed by color development with tetramethylbenzidine (TMB) substrate solution (as per the manufacturer's instructions) and the level of the colored reaction product was measured spectro-photometrically at 450 nm.

The MTT viability assay was performed with MTT-based In vitro Toxicology Assay Kit, (Sigma, MO, USA). MTT was first prepared as a stock solution of 5 mg/ in phosphate buffer (PBS, pH 7.2) and was filtered. At the end of the GLS-1027 treatment period (72 h.), 25 µl of MTT solution was added to each well. After incubation for 4 h. at 37 °C, 100 µl of solubilizing buffer (10% sodium dodecyl sulfate dissolved in 0.01HCL) was added to each well. After overnight incubation, the 96-well plate was

read by an enzyme-linked immunosorbent assay reader at 570 nm for absorbance density values to determine the cell viability. The viable cells produced a dark blue formazan product, whereas no such staining was formed in the dead cells. FACS analysis was performed to quantify apoptosis in experimental cells. At 72 h. post-drug treatment, Annexin-V staining was performed as recommended by the manufacturer (BD PharMingen, CA, USA) to quantify cell death. Cells were detached, double stained with FITC-conjugated Annexin V (BD PharMingen, CA, USA) and 1.25 μg/ml propidium iodide (Sigma, MO, USA) and analyzed by flow cytometry.

For surface staining, 5×10^6 cells were blocked with 50 μl of 20 μg/ml anti-CD16/32 (Bio Legend, CA, USA) for 15 min on ice. Cells were then incubated with 50 μl of appropriate antibodies for 30 min on ice. Biotinylated antibodies were detected by additionally staining with 100 μl of Brilliant Violet 510 Streptavidin (BD Biosciences, CA, USA) for 10 min on ice. 2% FBS was used as the diluent for each stain unless indicated otherwise. The concentration of antibodies and other reagents were used at manufacturer's recommend concentrations. Dead cells were excluded from the analysis by propidium iodide staining and live cells were gated on the basis of their forward scatter and side scatter characteristics and analyzed directly on a Coulter EPICS Flow Cytometer (Coulter, Hialeah, FL, USA) using FlowJo software (TreeStar, CA, USA). All samples were compared to their isotype-matched controls. In the case of dual flow cytometry individual samples treated with each isotype alone were used to determine the background levels of auto fluorescence [26, 29].

Cell lysates extracts preparation, ELISA analysis and Western blot analysis

For Western blot analysis, experimental cell pellets were thawed on ice and resuspended in ice-cold cell lysis buffer (Cell Signaling Technology, MA, USA). After incubation on ice for 5 min, the mixture was sonicated four times for 5 s each. The cell lysates were then centrifuged at 14,000 rpm at 4 °C for 10 min, and the supernatant was collected. After the protein concentration of the supernatant was measured with BCA assay the cell lysates were stored at − 80 °C until future use. Cell lysate (25 μg) proteins were separated by 12% SDS-PAGE and proteins were transferred to a nitrocellulose membrane. The membrane was washed for 5 min in Tris Buffer Saline plus Tween (TBST) buffer followed by incubation in blocking buffer for 1 h. at room temperature and subsequently treated with 1:1,000 dilutions of antibody in buffer (TBST with 0.5% BSA), overnight at 4 °C with rocking. Antibodies for Western blot analysis phosphorylated primary human antibodies specific to proteins: Phospho-IRAK1 (Thr209; cat. #12,756) and anti-total antibodies to IRAK1 antibody (cat. # 4359), were purchased from Cell Signaling Technology (Beverly, MA). Bands were visualized by autoradiography (Amersham Biosciences, NJ, USA). ELISA based phospho-TAK1 activity was determined using Phospho-TAK1 (S412) ELISA Kit (cat. # ab279950) from Abcam.

NF-κB luciferase, nuclear translocation assays

For determination of NF-κB inhibition, a reporter assay was performed. Briefly, transfections were conducted with 5 μγ of reporter plasmid (pNF-κB-Luc) or control plasmid (pTAL-Luc vector) (BD Biosciences, CA, USA) by using FuGENE 6 transfection Reagent (Roche Applied Science, IN, USA) in HeLa cells. To assess transfection efficiency, cells were co-transfected with β-galactosidase control vector (Promega, WI, USA). Transfected cells were treated with or without TNF-α (1 ng/ml) in the absence or presence of 1 μM or 10 μM GLS-1027. Two days post transfection the cells were washed twice in phosphate-buffered saline and total cell extracts prepared in 250 μl of reporter lysis buffer (RLB) according to the manufacturer's instructions (Promega, WI, USA). Cellular debris was removed by centrifugation and the luciferase activity of 50 μl of extract was read using LUMAT LB9501 (Berthold, Oak Ridge, TN, USA). Recombinant human TNF-α was obtained from R&D Systems (Minneapolis, MN, USA). All experiments were repeated at least twice. Reporter gene activity is reported as relative light units (RLU) which results from the ratio of luciferase units to β-gal units for each data point. β-galactosidase activity was determined using a Promega kit to verify the reproducibility between the quadruplicate transfections in all experiments. Error bars on transfection data represent the standard deviations of duplicate samples. In each control case, the luciferase activity was detectable, minimal, and significantly below all other data points.

^{3}H-thymidine uptake and ELISpot assays

Briefly, 2×10^5 PBMC were cultured in 96 well plates for 7 days in a media consisting of RPMI 1640 (Gibco–BRL) with 10% fetal calf serum (Gibco-BRL). A 100 μl aliquot containing 5×10^5 cells were immediately added to each well of a 96-well microtiter round bottom plate. Anti-CD3/CD28 (anti-CD3 (OKT3) was used at 1 μg (BioLegend, San Diego, CA) and anti-CD28 (CD28.2) at 2 μg (BioLegend, San Diego, CA) were added to wells in triplicate in presence of absence of GLS-1027 (10 μM). The cells were incubated at 37 °C in 5% CO_2 for 3 days. One μCi of tritiated thymidine was added to each well and the cells were incubated for 12–18 h. at 37 °C. Stimulation index (SI) was calculated form the formula SI = (Experimental count/spontaneous count). Spontaneous count

wells (media only) include 10% fetal calf serum. To assure that cells were healthy, Concanavalin A (Sigma) was used as a polyclonal stimulator positive control. SI was considered as positive when ≥ 3. ELISpot assay was performed to determine the frequency of interferon-γ (IFN-γ) secreting cells as described before [31].

Treatment and monitoring for diabetes by blood glucose measurement

Eight- to nine-week-old female NOD mice (approximately 20-25 g) were purchased from Jackson Laboratories (Bar Harbor, ME, USA) and housed under pathogen-free conditions at the Department of Biomedical and Biotechnological Sciences in the School of Medicine, at the University of Catania (Catania, Italy). All animals were acclimated for at least one week prior to initiation of dosing. Animals were randomized upon receipt and cages were subsequently randomized into treatment groups. All animal experiments were conducted in accordance with national and local regulations regarding animal welfare, and with the approval of the institutional animal care and use committee (IACUC) for the facilities that conducted the studies.

To study the impact of GLS-1027 under a late prophylactic regime, female NOD mice were treated once daily intraperitoneal injection (IP) with either vehicle or GLS-1027 (5 mg/mouse) from 10 to 20 weeks of age ($n = 16$ per group). Blood glucose was monitored using glucometers (ENCORE Glucometer, Bayer Corp., Elkhart, IN, USA) twice weekly, beginning at 10 weeks of age. Mice with blood glucose levels ≥ 11 mmol/L on two consecutive occasions were considered diabetic. Diabetic mice were sacrificed the day when diagnosis was confirmed.

In vivo cytokine levels in lymphocyte cultures and serum

Pancreatic lymph nodes and spleens were aseptically isolated from the euglycemic mice sacrificed at the end of the study. Organs were aseptically crushed to yield single-cell suspensions in culture medium that consisted of RPMI-1640 medium supplemented with 10% fetal bovine serum (FBS; Sigma, St. Louis, MO, USA), 2 mM L-glutamine, 10 mM HEPES, 1 mM sodium pyruvate, 100 U/ml penicillin, and 5 µg/ml streptomycin (GIBCO, Grand Island, NY, USA). After centrifuging spleen cell suspensions at 300 × g for 10 min, red blood cells were lysed with 3 ml of chilled red blood cell lysis buffer (Sigma) on ice for 5 min and then washed three times with chilled culture medium via centrifugation. Lymphocytes from lymph nodes (5×10^5/well) or a spleen (10^6/well) were cultured with Concanavalin A (Con A; 2.5 µg) in 1 ml of culture medium for 48 h., and conditioned medium was collected and stored at -80 °C until ELISA analysis of IL-17A (BioLegend, San Diego, CA, USA) levels. Serum samples were obtained from terminal blood samples collected immediately after CO_2 euthanasia and assessed for IL17A levels via ELISA.

Statistical analysis

Statistical analysis was conducted using GraphPad Prism, version 9 (GraphPad Software, CA, USA). Data are expressed in histograms as mean ± standard deviation. Comparison of groups was performed with a non-parametric two-tailed *t*-test (Mann–Whitney), and the relevant *p* values are indicated. Disease incidence is shown as percentage of diabetic-free animals in the experimental groups and Log-rank test was performed for significant differences. Ex vivo and in vivo levels of IL-17A are shown as mean ± standard deviation and two-tailed Student's t test was performed to assess the presence of significant differences among groups. For all the analyses a *p* value of < 0.05 was considered significant.

Results

GLS-1027 inhibits production of proinflammatory cytokines from monocytes and macrophages after stimulation of PRRs

To explore the mechanisms of actions of GLS-1027, we first investigated whether it could inhibit proinflammatory cytokines production by primary macrophages resultant from PRR stimulation. To establish that any effect(s) we observed was not due to GLS-1027 cytotoxicity, we cultured various cell lines (HeLa, U937, RD, Jurkat, and A549) and primary human $CD4^+$T cells in the presence of various concentrations of GLS-1027 100 µM, 10 µM, 1 µM, 0.1 µM or 0.01 µM of GLS-1027 and measured cell viability after 48 h. by MTT and Annexin-V FACS assay. The MTT and FACS assay results (Supplementary Fig. 1A-B) showed that the viability of each cell line and primary $CD4^+$T cells was stable over a five-log concentration range of GLS-1027 and remained above 80% even at the highest concentration tested, 100 µM, a concentration far above that deemed physiologic in published studies [14]. A panel of cell lines and human primary cells were stimulated with LPS in the absence or presence of GLS-1027 and levels of the pro-inflammatory cytokine TNF-α were measured in supernatants at 48 h. post stimulation. LPS treatment of primary monocytes, peripheral blood mononuclear cells (PBMCs), U937 (human monocytic cell line) and RAW 264.7 cells (mouse macrophage) induced strong secretion of TNF-α from these cells which was suppressed in the presence of GLS-1027 (Fig. 1A). By contrast, very little TNF-α was produced by primary $CD4^+$ T cells or the Jurkat T cell line after LPS treatment consistent with reports that they express either low levels or no TLR4 [32–34]. Activation of T cells by CD3/CD28 cross-linking was not affected by

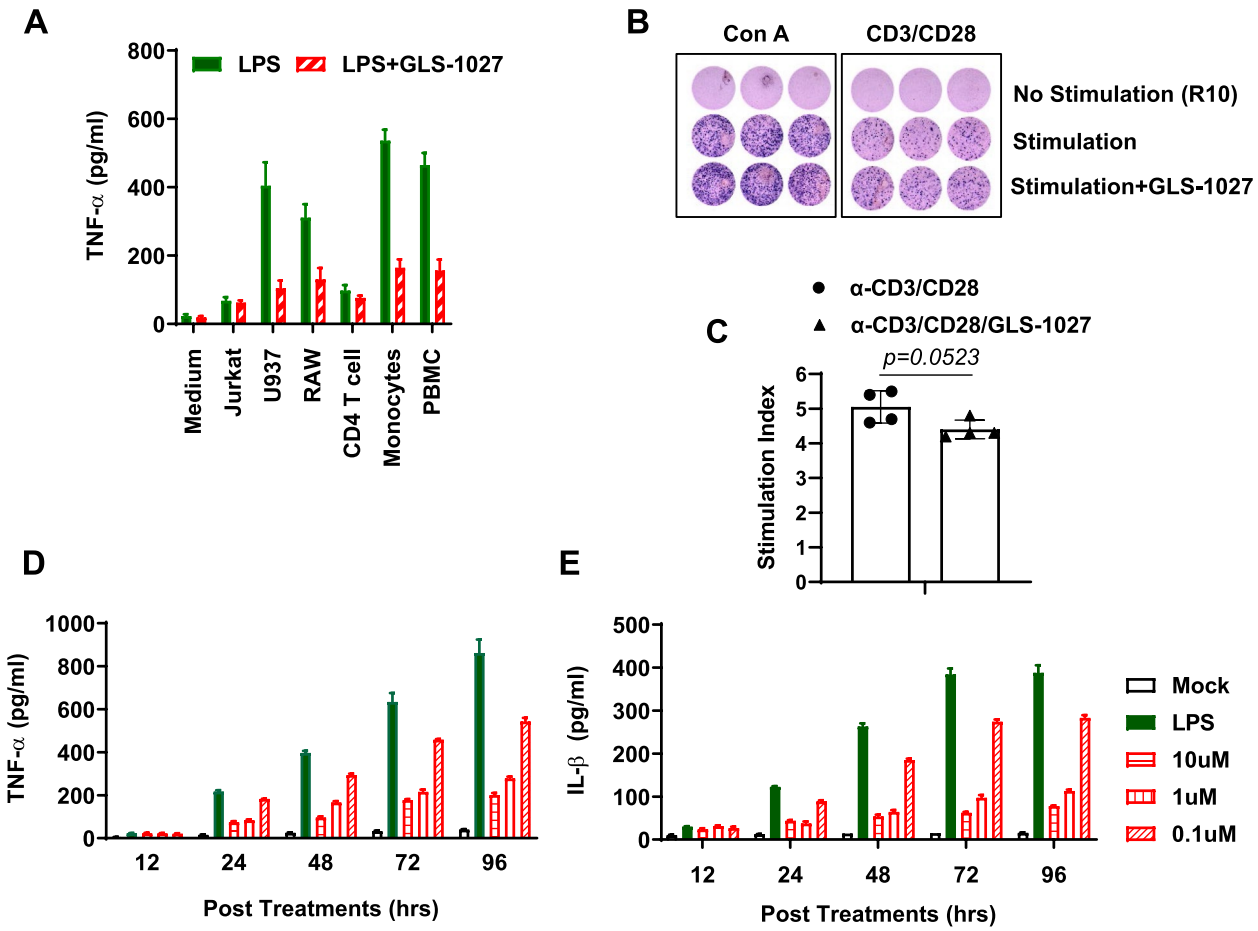

Fig. 1 GLS-1027 inhibits pro-inflammatory cytokine release in human PBMC in vitro. (**A**) GLS-1027 exhibits cell-type-specific inhibition of LPS-induced TNF-α production. TNF-α levels were measured 48 h post stimulation with LPS (5 μg/ml) in absence or presence of GLS-1027 (10 μM). (**B**) GLS-1027 does not inhibit CD3/CD28 mediated T cell activation. Purified human $CD3^+$ T cells were stimulated with anti-CD3/CD28 beads (10 μg/ml) or ConA in the presence or absence of GLS-1027 (10 μM), and IFN-γ production was measured via ELISpot immune assay. (**C**) T cell proliferation in the presence or absence of 10 μM GLS-1027 was analyzed by ^{3}H-thymidine uptake lymphoproliferative assay after co-stimulation through $CD3.^+CD28$ using plate bound antibodies. (**D-E**) GLS-1027 exhibits dose-dependent inhibition of TNF-α and IL-1β secretion from LPS-stimulated cells. PBMC were isolated and cultured in the presence or absence of LPS 5ug/ml with or without GLS-1027 (0.1,1.0 or 10 μM). Cytokine levels (pg/ml) in cell-free supernatants were assayed by ELISA as described under Materials and Methods. Error bars in all panels indicate 1 standard deviation among 3 replicates per condition. The experiment was repeated twice with similar results are shown in this representative experiment

GLS-1027 measured by either ELISpot or [30] thymidine uptake lymphoproliferative assays; (Fig. 1B-C). GLS-1027 inhibited LPS-induced production of the pro-inflammatory cytokines TNF-α and IL-1β from PBMCs in a dose dependent manner (Fig. 1D-E). These data show that GLS-1027 reduces pro-inflammatory cytokine production from monocyte and macrophage cells and cell lines following TLR4 stimulation but does not affect T cell activation.

GLS-1027 inhibits activation of NF-κB and p38 MAPK

Pro-inflammatory cytokine production following TLR engagement is mediated by the activation of transcription factors, so we investigated the effect(s) of GLS-1027 on activation of NF-κB family transcription factors and on p38 MAPK signaling which activates other transcription factors downstream of TLR signaling. Monocytes were stimulated with LPS in the presence of GLS-1027 had lower levels of phosphorylated NF-κB p65 than those stimulated with LPS alone as measured using flow cytometry (Fig. 2A). By contrast, there was no difference in levels of phosphorylated NF-κB p65 seen in monocytes stimulated with TLR3 agonist poly I:C in the absence or presence of GLS-1027 confirming previous reports that GLS-1027 targets only some PRRs [13, 16]. There was also decreased luciferase production seen

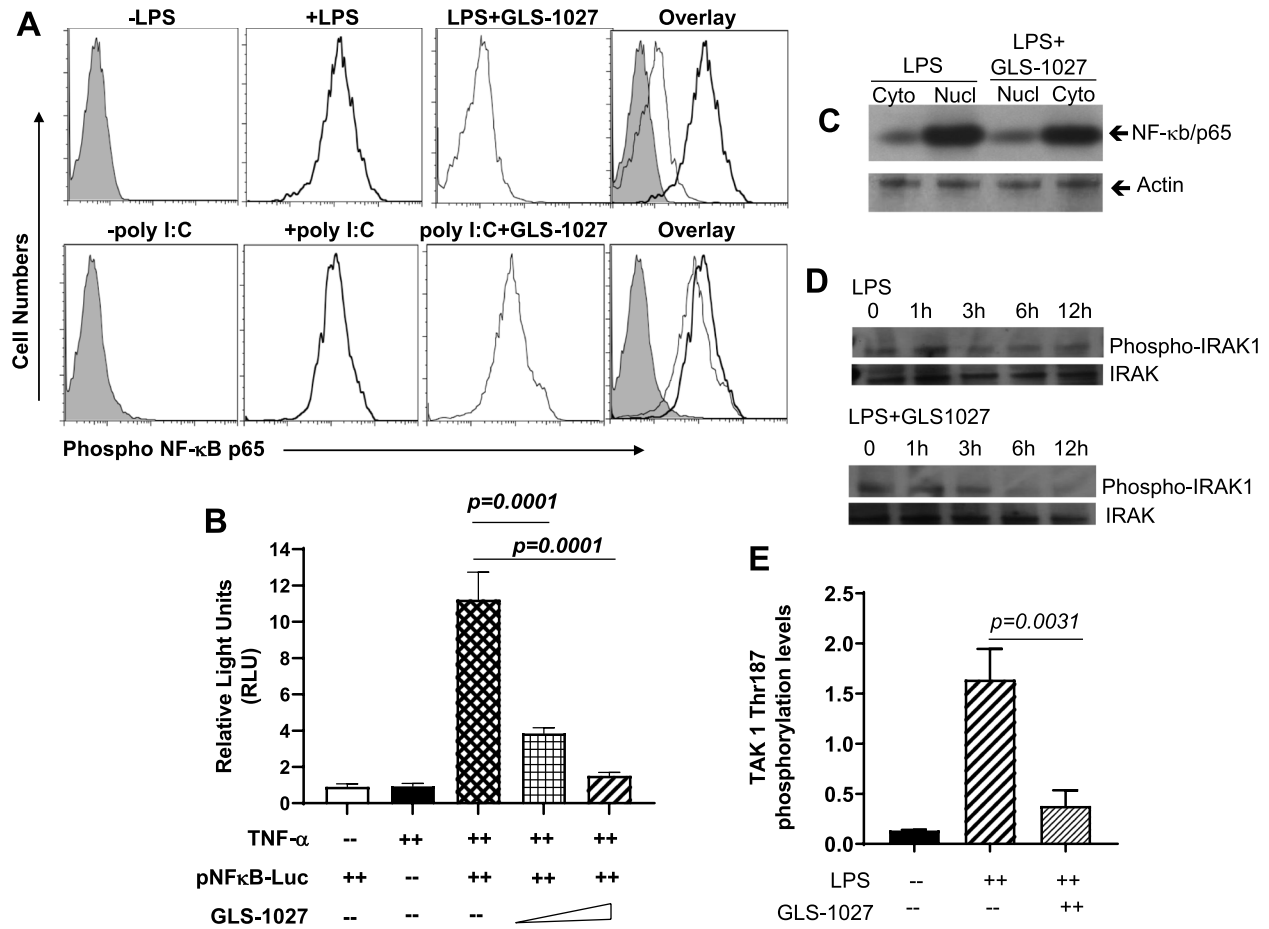

Fig. 2 GLS-1027 inhibits the activation of NF-κB and p38 pathways induced by LPS, but not by Poly(I:C). (**A**) Flow-cytometric analysis of phospho NF-κB -p65 in monocytes after LPS and poly I:C stimulation in the presence or absence of 10 μM of GLS-1027 in vitro. After stimulation, cells were fixed and permeabilized. The cells were stained with fluorochrome-conjugated antibodies against the CD14 monocyte cell surface marker and phospho NF-κB -p65. The CD14-positive monocyte population was analyzed for intracellular levels of phosphorylated NF-κB using flow cytometry with the data displayed as histograms. (**B**) Inhibition by GLS-1027 of NF-κB (p65) DNA binding activity in TNF-α stimulated cells. Nuclear extracts were obtained from unstimulated and TNF-α stimulated at indicated time points in the presence or absence of GLS-1027 (1 and 10 μM) cells and DNA-binding activity was examined by ELISA based EMSA assay. To confirm the specificity of this assay competitor oligo used as control. Data shown are representative of two independent experiments. (**C**) Cells were stimulated with TNF-α with or without GLS-1027 (10 μM) for 3-5 h. Cells were fixed and stained with an anti-NF-κB (p65) antibody, followed by anti-rabbit secondary antibody. (**D-E**) Phosphorylation of TAK1/IRAK1 is inhibited with GLS-1027. Human primary macrophages were treated with TNF-α and LPS, in the presence or absence of 10 μM of GLS-1027. The activation status of TAK1/IRAK was examined in the cell lysates by immunoblot analysis using the phospho-IRAK (T209) antibody (**D**) and phospho TAK1 activity was determined using ELISA (**E**), as described in Materials and methods

in HeLa cells transfected with a NF-κB responsive luciferase reporter gene system when they were stimulated with TNF-α in the presence of increasing concentrations of GLS-1027 (Fig. 2B). Furthermore, LPS treatment of primary human macrophages induced phosphorylation of IKK-α/β complex within five minutes, and GLS-1027 suppressed this LPS-mediated phosphorylation. Under resting conditions, NF-κB proteins are localized in the cytoplasm through binding to inhibitory IκB proteins [35]. Inflammatory stimuli promote the phosphorylation, ubiquitination, and subsequent proteasomal degradation of IκB proteins allowing the NF-κB family proteins to translocate into the nucleus where they can mediate gene transcription alone or in combination with other transcription factors. To evaluate the consequences of the reduced IKK-α/β complex phosphorylation, we generated protein fractions of macrophages stimulated with LPS in the absence or presence of GLS-1027 to see where p65 was localized. The decrease in p65 nuclear localization corresponded with decreased luciferase production from a NF-κB responsive luciferase reporter gene system in transfected HeLa cells that were stimulated with LPS

in the presence of increasing concentrations of GLS-1027 (Fig. 2C).

GLS-1027 affects the signaling cascade of MyD88-dependent TLRs

We next investigated the activation status of proteins involved in the signaling cascade downstream of TLRs that result in activation of p38 MAPK and NF-κB [36]. We focused on proteins involved in signaling mediated by the MyD88 adaptor protein as it is used by all the PRRs. Upon recruitment to a stimulated TLR, MyD88 recruits the IL-1 receptor-associated kinase-4 (IRAK-4) to the TLR which then phosphorylates and activates IRAK-1 [36, 37]. After IRAK-1 becomes phosphorylated, it forms a complex with two membrane-bound proteins, TAB2 and TRAF6, and this complex then activates downstream protein kinase cascades including that mediated by TAK1. Activated TAK1 phosphorylates IKKα/β, MKK3/6, and MKK4/7 which activates the NF-κB, p38 MAPK and JNK pathways respectively, and these pathways promote the active transcription of inflammatory cytokines [37]. TAK1 is also activated downstream of NOD 1 and 2 as well as other cytokine receptors. Signaling downstream of TRIF utilizes another pathway to phosphorylate NF-κB that does not involve activation of IRAKs or TAK1 [32, 37].

To investigate the effects of GLS-1027 on MyD88-dependent signaling, lysates were collected from primary human macrophages stimulated with LPS in the absence or presence of GLS-1027 and evaluated by Western analyses. LPS treatment stimulated IRAK-1 phosphorylation in macrophages within an hour while GLS-1027 suppressed this (Fig. 2D). Treatment of primary human macrophages with LPS also initiated strong phosphorylation of TAK1 (Fig. 2E), and this phosphorylation was reduced but not fully eliminated by GLS-1027. GLS-1027 was able to reduce TAK-1 phosphorylation mediated by TLR or cytokine receptor signaling. These results show that GLS-1027 attenuates multiple activation steps in the signaling cascade downstream of TLRs which can contribute to the reduced activation of p38 MAPK and NF-κB transcription. These results show that GLS-1027 modulates inflammation in part through preventing activation of NF-κB transcription factors and p38 MAPK activity downstream of select pattern recognition receptors (PRRs).

GLS-1027 inhibits maturation of dendritic cells

Dendritic cells link the initial innate immune response to inflammatory stimuli with the development of adaptive immune responses that can help resolve the inflammation. Immature dendritic cells reside in various tissues where they scavenge for foreign material and stay receptive for stimulatory signals from pathogen-associated molecular patterns (PAMPs), damage-associated molecular patterns (DAMPs), and other signals [38]. Upon capture of a foreign agent and receipt of stimulatory signals, immature DCs undergo a maturation process where they down regulate their antigen internalization functions and up-regulate their antigen presenting functions. We evaluated if GLS-1027 affects dendritic cell maturation. Mature DCs were developed by culturing monocytes with GM-CSF and IL-4. Immature DCs were stimulated with LPS in the absence or presence of GLS-1027 and evaluated by flow cytometry for the upregulation of MHC and co-stimulatory molecules indicative of maturation. As shown in Fig. 3A, LPS stimulation promoted the expression of HLA-DR as well as the co-stimulatory molecules CD83 and CD86 on DCs, but the expression of all three molecules was reduced when GLS-1027 was present. Supernatants from DCs cultured with LPS in the presence of GLS-1027 had significantly less pro-inflammatory cytokines including IL-6, IL-1β, TNF-α, and IL-23 (Fig. 3B). These data show that GLS-1027 inhibits dendritic cell maturation and reduces their secretion of pro-inflammatory cytokines.

GL-1027 inhibits development of Th17 cells

We also evaluated the effect(s) of GLS-1027 on the differentiation of $CD4^+$ T cells into Th17 cells. Purified, naïve human $CD4^+$ T cells were cultured with or without Th17-inducing cytokines for 6 days following the protocol of Zhou, L. et al. on Th17 cell differentiation [39]. In some cultures, GLS-1027 was added at a concentration of 1 μM or 10 μM at the same time as the Th17-inducing cytokines. After six days of culture, this cytokine mix produces cells classically defined as Th17 cells which includes a $CD4^+CD45RO^+CCR6^+$ phenotype and the production of INF-γ and IL-17 by FACS analysis and IL-17 secretion was measured by ELISA after IL-1β stimulation (Supplementary Fig. 1C-D). After six days cells from the various cultures were stimulated with IL-1β and production of IL-17 was measured in Th17 cells produced in the absence or presence of GLS-1027 by flow cytometry. As seen in Fig. 4A-B, GLS-1027 prevented in a dose dependent manner the development of $CD4^+$ T cells that produce IL-17 upon IL-1β stimulation. Cells differentiated in the presence of 10 μM GLS-1027 also secreted significantly less IL-17 and IL-23 (Fig. 4C-D). This result shows that GLS-1027 directly affects development of Th17 cells independently of its effects on monocytes and dendritic cells which are upstream mediators in the inflammation cascade.

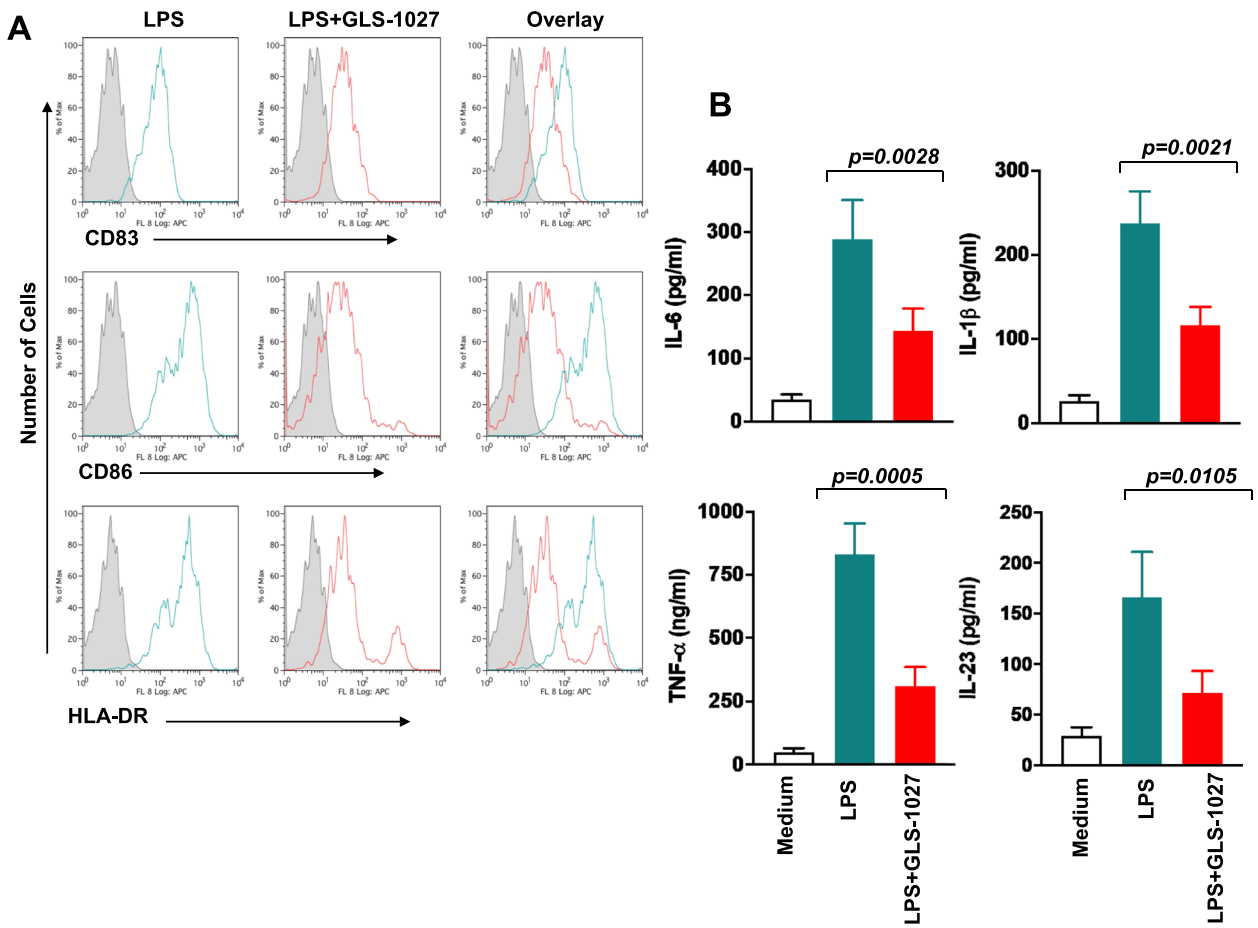

Fig. 3 Effect of GLS-1027 on DC's differentiation and maturation. (**A**) Fresh human monocytes were allowed to attach to cell culture plates as described in Materials and Methods and stimulated with GM-CSF/IL-4 for 6 days were allowed to adhere in the absence or presence of GLS-1027 (10μM) for 7 days to develop into dendritic cells. On day 7, the cells were harvested, and were stained with indicated mAbs and analyzed by flow cytometry. Histograms show the staining of specific surface markers, and filled grey histograms represent the isotype-matched control antibody staining, blue line is LPS treatment, and red line is LPS + GLS-1027 treatment. The results are representative of two independent experiments. (**B**) GLS-1027 inhibits LPS-induced cytokine production of DCs. On day 7 cell culture supernatants from DCs cultured with LPS in the presence of GLS-1027 were measured via ELISA for the concentrations of the cytokines TNF-α, IL-1β, IL-6 and IL-23 in the media. A non-parametric two-tailed *t*-test (Mann–Whitney) was used for statistical analysis, and the relevant *p* values are indicated. Error bars in all panels indicate 1 standard deviation among 3 replicates per condition. The experiment was repeated twice with similar results are shown

Modulation of pathogenic T cell phenotype by treatment with GLS-1027

To determine whether GLS-1027 could effectively suppress spontaneous onset of diabetes in female NOD mice, single daily doses of GLS-1027 (5 mg/mouse) or vehicle were administered intraperitoneally in euglycaemic mice at 10 weeks of age and continued through 20 weeks of age. The first incidence of diabetes was observed at week 13 and the peak of incidence was reached at week 18 of age, when the incidence in the vehicle-treated cohort was 56.3% and in the GLS-1027-treated cohort was 18.8% ($p = 0.038$ by Log-rank test) (Fig. 5A). After dosing with vehicle or GLS-1027, the euglycemic mice were sacrificed at the end of the treatment period, and pancreatic lymph nodes and spleen were isolated. Cells were cultured with conditioned medium was analyzed for levels of IL-17A (Th17 phenotype) and TNF-α. Treatment with GLS-1027 led to a significant reduction in IL-17A production by both splenocyte ($p < 0.01$ by two-tailed Student's t test) and pancreatic lymph node cultures ($p < 0.001$ by two-tailed Student's t test) (Fig. 5B). The suppressive effect of GLS-1027 on Th17 polarization was also apparent with serum IL-17A levels, as significantly diminished levels could be observed in the serum of GLS-1027-treated mice, as compared to vehicle-treated animals ($p < 0.01$) (Fig. 5C). These results demonstrate that the

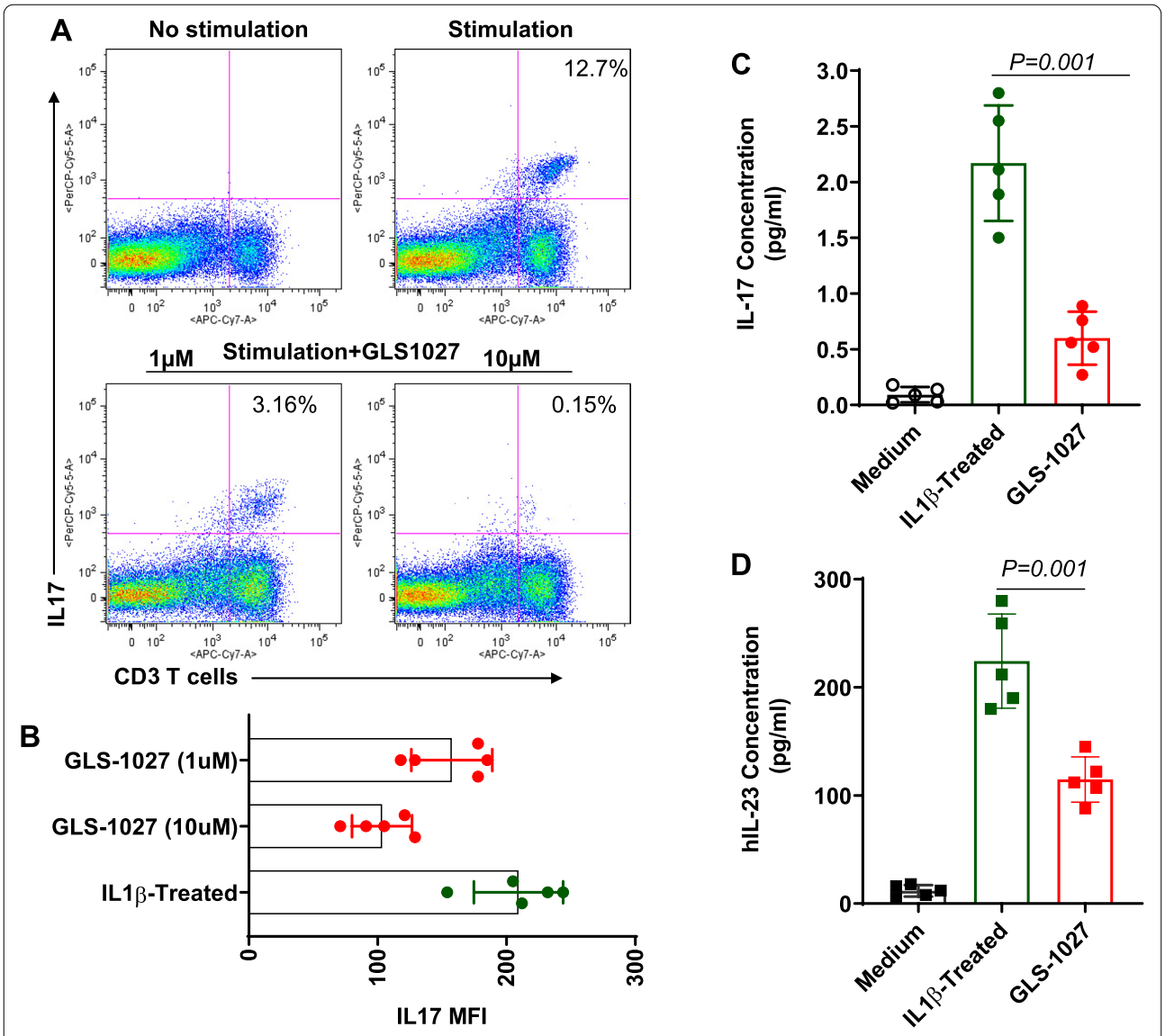

Fig. 4 GLS-1027 prevents the development of Th17 T cells. Purified, naïve human CD3 T cells from peripheral blood mononuclear cells (PBMC) by depleting B cells, NK cells, monocytes, platelets, dendritic cells, granulocytes, and erythrocytes. Isolated $CD3^+$ T cells were bead- and antibody-free and incubated with 10 U/ml of IL-2, 10 ng/ml of IL-1β, 10 ng/ml of IL-23, 1ug/ml of anti-IL-4, 1ug/ml of anti-IFN-γ and anti-CD3/CD28 activation beads at a ratio of 1 bead per cell plus IL1-β 10ng/ml. In some cultures, GLS-1027 was added at a concentration of 1μM or 10μM at the same time as the Th17-inducing cytokines. (**A**) On day 6, the cells were stained with antibodies to CD4 and intracellular IL-17A and then evaluated by flow cytometry. Percentage of $CD4^+/IL\text{-}17^+$ cells indicated in the upper right quadrant of plots. (**B**) Mean Fluorescent Intensity (MFI) of IL-17 in $CD4^+$ T cells. (**C-D**) Concentration of IL-17 and IL-23 in media of differentiated $CD4.^+$ T cells; GLS-1027 concentration was 10μM. A non-parametric two-tailed *t*-test (Mann–Whitney) was used for statistical analysis, and the relevant *p* values are indicated. Error bars in all panels indicate a standard deviation among 3 replicates per condition. The experiment was repeated twice with similar results are shown in this representative experiment

efficacy of GLS-1027 is associated with down-regulation of the pathogenic Th17 autoimmune responses, suggesting an immunoregulatory function of the drug. Also, the immune-suppressive effect of GLS-1027 was apparent from the significant reduction of TNF- α production by both splenocytes ($p < 0.001$) and lymph node cells ($p < 0.01$) (Fig. 5D), as well as from the reduced levels of serum TNF-α in GLS-1027-treated mice, as compared to vehicle-treated animals ($p < 0.01$) (Fig. 5E).

Discussion

Here we show that GLS-1027 modulates inflammation through both cell-autonomous and non-cell autonomous effects on several cell types involved in inflammation.

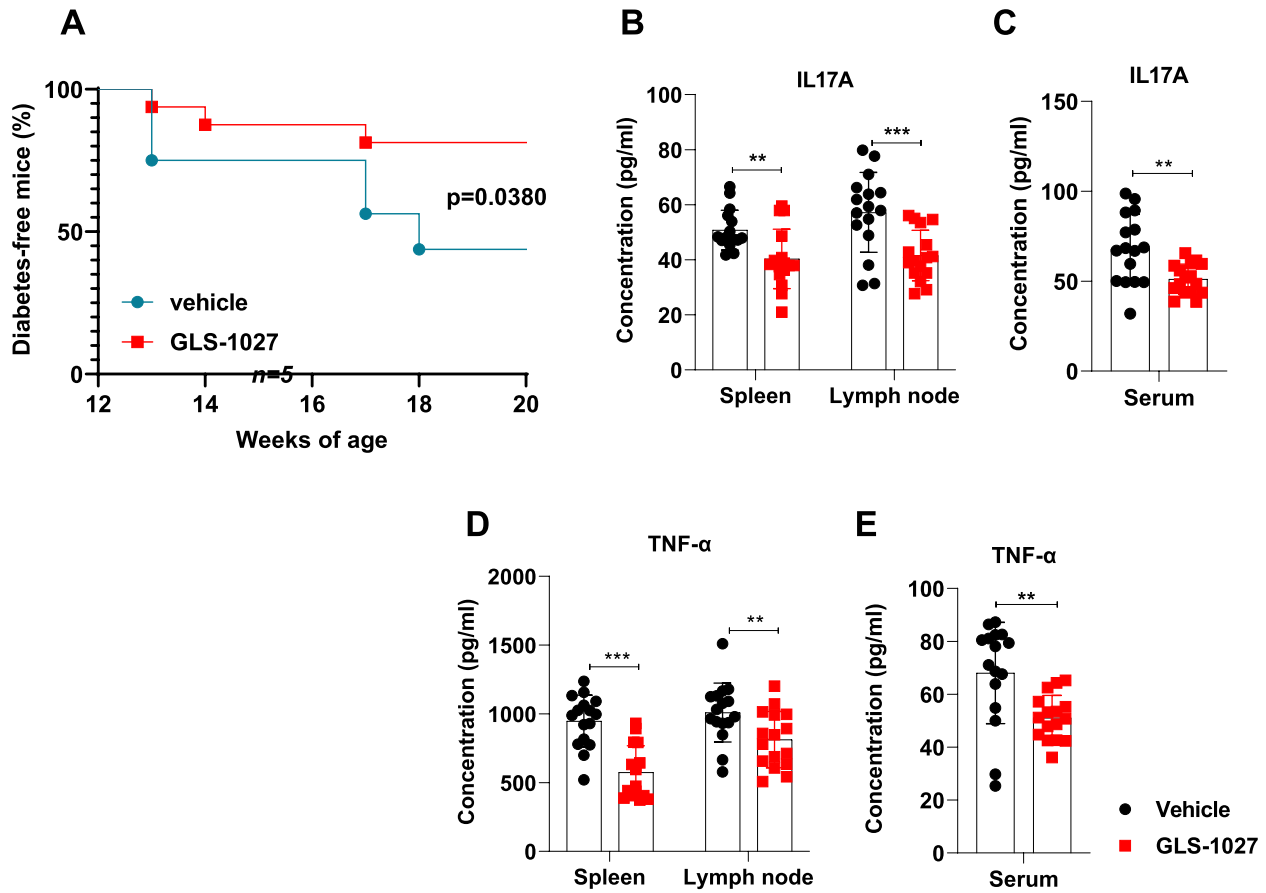

Fig. 5 GLS-1027 prevents type 1 diabetes in the NOD mouse. **(A)** Eight to nine weeks-old female NOD mice were treated with GLS-1027 (5 mg/mouse) under a late prophylactic regime, from 10 to 20 weeks of age ($n = 16$ per group). Blood glucose was monitored and mice with blood glucose levels ≥ 11 mmol/L on two consecutive occasions were considered diabetic. Diabetic mice were sacrificed the day when diagnosis was confirmed. **(B)** Spleens and pancreatic lymph nodes were aseptically isolated from the mice and cells from spleen (10^6/well) or lymph nodes (5×10^5/well) were cultured with Concanavalin A (Con A; 2.5 µg/ml) in the of culture medium for 48 h. The concentration of IL-17A in the culture media was measured by ELISA. **(C)** Serum samples were obtained from terminal blood samples collected immediately after CO_2 euthanasia and assessed for IL-17A levels via ELISA. **(D)** Spleens and pancreatic lymph nodes were aseptically isolated from the mice and cells from spleen (10^6/well) or lymph nodes ($5 \times 10.^5$/well) were cultured with Concanavalin A (Con A; 2.5 µg/ml) in 1 ml of culture medium for 48 h. The concentration of TNF-α in the culture media was measured by ELISA. **(E)** Serum samples were obtained from terminal blood samples collected immediately after CO_2 euthanasia and assessed for TNF-α levels via ELISA. Treatment with GLS-1027 resulted in a dose-dependent inhibition of cytokines. Error bars in all panels indicate 1 standard deviation among 3 replicates per condition

It can reduce secretion of pro-inflammatory cytokines after stimulation of PRRs from innate immune cells such as monocytes and macrophages that are often the first cells to respond to an inflammatory stimulus. GLS-1027 appears to target PRRs and cytokine receptors such as IL-1 receptor (IL-1R) that use the MyD88 adaptor protein as it had no effect on cytokine production in cells treated with an agonist for TLR3 which uses the TRIF adaptor protein to stimulate NF-κB activation. GLS-1027 also had no effect on T cell proliferation mediated by activation of T cell receptor signaling by anti-CD3/CD28 antibody crosslinking. The GLS-1027-mediated reduction in cytokine production correlated with decreased activation of NF-κB family transcription factors. GLS-1027 also impeded maturation of dendritic cells and differentiation of Th17 cells which resulted in decreased production of pro-inflammatory cytokines from these cell types [40, 41]. In vivo, daily doses of GLS-1027 impeded development of diabetes in susceptible NOD mice and lowered levels of the proinflammatory cytokine IL-17A in treated mice.

In a previous paper, gene expression in PBMCs stimulated with LPS in the presence or absence of GLS-1027 was studied using a genome-wide oligonucleotide microarray [13]. GLS-1027 modulated the expression of several genes in LPS-stimulated PBMCs, particularly, those

genes involved in antigen processing and presentation, graft-versus-host disease, spliceosome, and systemic lupus erythematosus. This decrease in gene expression may be explained in part by the decreased activation of both NF-κB transcription factors in GLS-1027-treated, LPS-stimulated cells seen in this study. GLS-1027-mediated inhibition of gene expression likely also contributed to the inhibition of DC maturation and Th17 cell development as both of those processes require activation of gene expression resultant from stimulation of cytokine receptors and PRRs. The ability of GLS-1027 to suppress Th17 cell development is interesting, and likely important as it inhibits multiple arms required for Th17 genesis. While GLS-1027 can work directly on naïve CD4 T cells to prevent their maturation into Th17 cells it can also impede their development through inhibiting maturation of DCs which provide cytokine and co-stimulatory signals that support CD4 T cell differentiation. In this way GLS-1027 may act as a global inhibitor of inflammation through inhibiting early activation by innate immune cells to inflammatory stimuli which reduces subsequent development of adaptive immune responses that could exacerbate the inflammation.

Genetic experiments have shown that these enzymes are necessary for basic physiological functions; loss of NF-κB function leads to embryonic lethality associated with massive liver degeneration; and hepatocyte-specific loss of p38α cooperates with NF-κB inhibition to lead to endotoxin-induced liver damage [42]. By working on the signaling pathway(s) downstream of select PRRs or cytokine receptors, the effects of GLS-1027 on gene-expression would not be expected to affect other mechanisms that stimulate NF-κB and p38 activity. In this study, minimal toxicity was seen in cells cultured with 100 mM of GLS-1027 which far exceeds the concentration deemed physiologic in published studies [13–15, 23]. This criterion has not been achieved with traditional NF-κB inhibitors, and thus may contribute to their undesirable toxicity such as elevated plasma transaminase levels [43, 44].

To link this immunopharmacological characterization of GLS-1027 to the in vivo setting, we studied its effects on the development of type 1 diabetes (T1D) in the non-obese diabetic [41] mouse model, a validated model of human type 1 diabetes [45, 46]. As seen in most cases of human type 1 diabetes, the diabetogenic potential of autoreactive T cells and macrophages infiltrating the beta cells during the insulitis process is mediated by their capacity to secrete Th1 and Th17 pro-inflammatory cytokines such as IL-1β [47–50], IFN-α [51, 52] and IL-18 [53] from islet-infiltrating leukocytes. Several, though not all, lines of evidence suggest a strong role for IL-17A in the autoimmune diabetogenic process in NOD mice and humans. IL-17A may trigger the upregulation of inducible nitric oxide synthase (iNOS) mRNA and protein expression in the MIN6β cell line and cause nitric oxide-dependent toxicity [20]. Immune cells can also infiltrate into exocrine glands such as salivary glands and lacrimal glands of NOD/LtJ mice to produce IL-17A, which destroys local glandular tissue and aggravates T1DM-associated Sjogren's syndrome. Increasing evidence also points to upregulated production of IL-17A both in the periphery and in beta cells affected by insulitis in patients with newly diagnosed human type 1 diabetes [54, 55]. However, there still exist some contrary or contradictory findings of the function of IL-17A and Th17 cells in T1D. One study found that patients with recent-onset T1D (less than 6 months of diagnosis) exhibited lower expression of IL-17RA in $CD3^+$ T and $CD4^+$ T cells and lower number of IL-17RA in $CD4^+$ T cells than controls [56]. That means, the IL-17A pathway possibly does not activate in the peripheral blood of newly diagnosed T1DM patients. Reasons for these discrepant results remain to be studied but may be related to different sampling conditions, inclusion criteria, different genetic backgrounds, or other confounding variables. The current lines of evidence supports the concept that upregulated IL-17 immunity occurs both in NOD mice and human T1DM and that IL-17A may represent a new therapeutic target for the prevention and possibly early treatment of the disease. We have shown here that administration of GLS-1027 to female NOD mice produced a significant delay in the progression of type 1 diabetes mellitus. Reduction in disease incidence was associated with a significant reduction of IL-17A production by spleen and lymph node cells and reduced IL-17A levels in serum. Overall, it seems likely that the capacity of GLS-1027 to downregulate IL-17A production may reflect an important immunopharmacological mechanism that suppresses the development and progression of type 1 diabetes mellitus in NOD mice.

While biologics such as monoclonal antibody treatments have shown remarkable efficacy for the treatment of inflammatory diseases, targeting of only a single molecule may limit efficacy in some conditions. Several diseases require inhibition of multiple factors for a meaningful reduction of clinical symptoms; for example, a third of Crohn's disease patients do not respond to anti-TNF-α therapy and many uveitis patients are resistant to steroid and/or immunosuppressive therapy. Instead of targeting a specific cytokine, GLS-1027 globally reduces production of multiple pro-inflammatory cytokines including IL-6, TNF-α and IL-1β which could help it ameliorate diseases where multiple cytokines are causing pathology. Most autoimmune disorders are now believed to be driven by hyperactive and/or production of Th17 T cells. Th17 cells are highly abundant in the tissues of

patients suffering from autoimmune disorders and are necessary for several autoimmune disorders in mice. Currently, there are no direct small molecule inhibitors of Th17 cells, although anti-p40 biologics (ABT-874 and CNTO-1275), which target the p40 subunit of both IL-12 and IL-23, were recently approved in the US [57]. Our data suggest that GLS-1027 inhibits multiple steps in the inflammatory cascade including dampening the initial response by innate immune cells to inflammatory stimuli and impeding directly and indirectly the development of adaptive immune responses to the inflammatory stimuli. Therefore, these data support the use of GLS-1027 for evaluation as treatment of autoimmune and inflammatory disorders due to Th17 T immunopathology.

Supplementary Information

The online version contains supplementary material available at https://doi.org/10.1186/s41231-022-00121-9.

Additional file 1: Figure S1 (A-B) GLS-1027 is non-cytotoxic. (A) Cell viability was examined in cell lines (HeLa, RD, Jurkat, A549 and U937) and primary $CD4^+$T cells after 48 hrs. of cell culture in the presence of 0.01, 0.1, 1, 10, or 100mM GLS-1027 by MTT assay to investigate the potential cytotoxicityof GLS-1027 (B) Cell viability of PBMC's was measured via PI/Annexin V staining after 48 hrs of cell culture in the presence of 10 or 100mM GLS-1027. (C-D) *In vitro* generation, differentiation, and expansion of Th17cells. Purified human $CD3^+$ T cells ($CD3^+CD4^+CD45RA^+CD25^-$HLA-DR^-) were incubated with 10 U/ of IL-2, 10ng/ml of IL-1β, 10ng/ml of IL-23, 1ug/ml of anti-IL-4, 1ug/ml of anti-IFN-γ and anti-CD3/CD28 activation beads at aratio of 1 bead per cell plus IL1-β (1ng/ml). On day 6, the cells were activated for 4 hrs in the presence of 50ng/ml of PMA, 500ng/ml of ionomycin. The cells were analyzed for intracellular staining of IL-17A and IFN-γ. In the presence of TGF-β & IL1β, 1% to 5% of $IL\text{-}17^+$ cells are typically observed by Flow cytometry analysis and cytokines in the supernatant were measured by ELISA. The experiment was repeated twice with similar results.

Acknowledgements
The authors would like to acknowledge the University of Pennsylvania School of Medicine Flow Cytometry Facility and Imaging Facility for their technical assistance.

Disclosure
SK, MJ, CCR, HL, YC, AG, YO, BJ, GJP, YKP, JNM, and KM are employees of GeneOne Life Sciences, Inc. The other authors declare no competing financial interests.

Authors' contributions
Conceptualization: Ferdinando Nicoletti and Kar Muthumani. Data curation: Sagar Kudchodkar, Paolo Fagone, Omkar U. Kawalekar, Ferdinando Nicoletti, Kar Muthumani. Formal analysis: Paolo Fagone, Omkar U. Kawalekar, Ferdinando Nicoletti, Kar Muthumani. Methodology: Sagar Kudchodkar, Paolo Fagone, Omkar U. Kawalekar, Ferdinando Nicoletti, Kar Muthumani. Resources: Moonsup Jeong, Christine C. Roberts, Hyojin Lee, Youngran Cho, Areum Gil, Yeeun Oh, Bohyun Jeon, Gee Ho Park, Young K. Park, Ferdinando Nicoletti, Joel N. Maslow, Kar Muthumani. Supervision: Ferdinando Nicoletti, Kar Muthumani. Writing original draft: Sagar Kudchodkar, Paolo Fagone, Omkar U. Kawalekar and Kar Muthumani. Writing review & editing: Sagar Kudchodkar, Ferdinando Nicoletti, Joel N. Maslow and Kar Muthumani. The author(s) read and approved the final manuscript.

Funding
Not applicable.

Availability of data and materials
The authors confirm that the data supporting the findings of this study are available within the article.

Declarations

Ethics approval and consent to participate
Not applicable.

Consent for publication
The authors listed participated in the preparation and approved the manuscript for publication.

Competing interests
The authors declare no competing financial interest.

Author details
[1]GeneOne Life Science Inc, Yeongdeungpo Gu, Seoul 07335, Korea. [2]Dept of Pathology and Lab Medicine, University of Pennsylvania, Philadephia, PA 19104, USA. [3]Department of Biomedicine and Biotechnology, School of Medicine, University of Catania, Catania, Italy.

Received: 12 January 2022 Accepted: 13 June 2022
Published online: 16 July 2022

References

1. Zheng D, Liwinski T, Elinav E. Inflammasome activation and regulation: toward a better understanding of complex mechanisms. Cell Discovery. 2020;6:36.
2. Karin M, Greten FR. NF-κB: linking inflammation and immunity to cancer development and progression. Nat Rev Immunol. 2005;5:749–59.
3. Leslie M. Inflammation's stop signals. Science. 2015;347:18–21.
4. Seong SY, Matzinger P. Hydrophobicity: an ancient damage-associated molecular pattern that initiates innate immune responses. Nat Rev Immunol. 2004;4:469–78.
5. Brown GD. Immunology: Actin' dangerously. Nature. 2012;485:589–90.
6. Ganguly D, Haak S, Sisirak V, Reizis B. The role of dendritic cells in autoimmunity. Nat Rev Immunol. 2013;13:566–77.
7. Kawai T, Akira S. The role of pattern-recognition receptors in innate immunity: update on Toll-like receptors. Nat Immunol. 2010;11:373–84.
8. Chou RC, Kim ND, Sadik CD, Seung E, Lan Y, Byrne MH, Haribabu B, Iwakura Y, Luster AD. Lipid-cytokine-chemokine cascade drives neutrophil recruitment in a murine model of inflammatory arthritis. Immunity. 2010;33:266–78.
9. Constantinides MG, McDonald BD, Verhoef PA, Bendelac A. A committed precursor to innate lymphoid cells. Nature. 2014;508:397–401.
10. Gleeson M, Bishop NC, Stensel DJ, Lindley MR, Mastana SS, Nimmo MA. The anti-inflammatory effects of exercise: mechanisms and implications for the prevention and treatment of disease. Nat Rev Immunol. 2011;11:607–15.
11. Sabado RL, Balan S, Bhardwaj N. Dendritic cell-based immunotherapy. Cell Res. 2017;27:74–95.
12. Karki R, Sharma BR, Tuladhar S, Williams EP, Zalduondo L, Samir P, Zheng M, Sundaram B, Banoth B, Malireddi RKS, et al. Synergism of TNF-alpha and IFN-gamma Triggers Inflammatory Cell Death, Tissue Damage, and Mortality in SARS-CoV-2 Infection and Cytokine Shock Syndromes. Cell. 2021;184(149–168): e117.
13. Fagone P, Muthumani K, Mangano K, Magro G, Meroni PL, Kim JJ, Sardesai NY, Weiner DB, Nicoletti F. VGX-1027 modulates genes involved in lipopolysaccharide-induced Toll-like receptor 4 activation and in a murine model of systemic lupus erythematosus. Immunology. 2014;142:594–602.
14. Stojanovic I, Cuzzocrea S, Mangano K, Mazzon E, Miljkovic D, Wang M, Donia M, Al Abed Y, Kim J, Nicoletti F, et al. In vitro, ex vivo and in vivo immunopharmacological activities of the isoxazoline compound VGX-1027: modulation of cytokine synthesis and prevention of both organ-specific and systemic autoimmune diseases in murine models. Clin Immunol. 2007;123:311–23.

15. Mangano K, Sardesai NY, Quattrocchi C, Mazzon E, Cuzzocrea S, Bendtzen K, Meroni PL, Kim JJ, Nicoletti F. Effects of the immunomodulator, VGX-1027, in endotoxin-induced uveitis in Lewis rats. Br J Pharmacol. 2008;155:722–30.
16. Mangano K, Sardesai N, D'Alcamo M, Libra M, Malaguarnera L, Donia M, Bendtzen K, Meroni P, Nicoletti F. In vitro inhibition of enterobacteria-reactive CD4+CD25- T cells and suppression of immunoinflammatory colitis in mice by the novel immunomodulatory agent VGX-1027. Eur J Pharmacol. 2008;586:313–21.
17. Stosic-Grujicic S, Cvetkovic I, Mangano K, Fresta M, Maksimovic-Ivanic D, Harhaji L, Popadic D, Momcilovic M, Miljkovic D, Kim J, et al. A potent immunomodulatory compound, (S, R)-3-Phenyl-4,5-dihydro-5-isoxazole acetic acid, prevents spontaneous and accelerated forms of autoimmune diabetes in NOD mice and inhibits the immunoinflammatory diabetes induced by multiple low doses of streptozotocin in CBA/H mice. J Pharmacol Exp Ther. 2007;320:1038–49.
18. Saurus P, Kuusela S, Lehtonen E, Hyvonen ME, Ristola M, Fogarty CL, Tienari J, Lassenius MI, Forsblom C, Lehto M, et al. Podocyte apoptosis is prevented by blocking the Toll-like receptor pathway. Cell Death Dis. 2015;6: e1752.
19. Min HS, Kim JE, Lee MH, Song HK, Lee MJ, Lee JE, Kim HW, Cha JJ, Hyun YY, Han JY, et al. Effects of Toll-like receptor antagonist 4,5-dihydro-3-phenyl-5-isoxasole acetic acid on the progression of kidney disease in mice on a high-fat diet. Kidney Res Clin Pract. 2014;33:33–44.
20. Xu M, Li F, Wang M, Zhang H, Xu L, Adcock IM, Chung KF, Zhang Y. Protective effects of VGX-1027 in PM2.5-induced airway inflammation and bronchial hyperresponsiveness. Eur J Pharmacol. 2019;842:373–83.
21. Zhang J-l, Huang W-m, Zeng Q-y. Atractylenolide I protects mice from lipopolysaccharide-induced acute lung injury. Eur J Pharmacol. 2015;765:94–9.
22. Upadhyay R, Ying WZ, Nasrin Z, Safah H, Jaimes EA, Feng W, Sanders PW, Batuman V. Free light chains injure proximal tubule cells through the STAT1/HMGB1/TLR axis. JCI Insight. 2020;5(14):e137191.
23. Lee JC, Menacherry S, Diehl MC, Giffear MD, White CJ, Juba R, Bagarazzi ML, Muthumani K, Boyer J, Agarwal V, et al. Safety, bioavailability, and pharmacokinetics of VGX-1027-A novel oral anti-inflammatory drug in healthy human subjects. Clin Pharmacol Drug Dev. 2016;5:91–101.
24. Muthumani K, Choo AY, Zong WX, Madesh M, Hwang DS, Premkumar A, Thieu KP, Emmanuel J, Kumar S, Thompson CB, Weiner DB. The HIV-1 Vpr and glucocorticoid receptor complex is a gain-of-function interaction that prevents the nuclear localization of PARP-1. Nat Cell Biol. 2006;8:170–9.
25. Manel N, Unutmaz D, Littman DR. The differentiation of human T(H)-17 cells requires transforming growth factor-beta and induction of the nuclear receptor RORgammat. Nat Immunol. 2008;9:641–9.
26. Muthumani K, Choo AY, Hwang DS, Premkumar A, Dayes NS, Harris C, Green DR, Wadsworth SA, Siekierka JJ, Weiner DB. HIV-1 Nef-induced FasL induction and bystander killing requires p38 MAPK activation. Blood. 2005;106:2059–68.
27. Muthumani K, Choo AY, Hwang DS, Dayes NS, Chattergoon M, Mayilvahanan S, Thieu KP, Buckley PT, Emmanuel J, Premkumar A, Weiner DB. HIV-1 Viral protein-r (Vpr) protects against lethal superantigen challenge while maintaining homeostatic T cell levels in vivo. Mol Ther. 2005;12:910–21.
28. Muthumani K, Hwang DS, Choo AY, Mayilvahanan S, Dayes NS, Thieu KP, Weiner DB. HIV-1 Vpr inhibits the maturation and activation of macrophages and dendritic cells in vitro. Int Immunol. 2005;17:103–16.
29. Muthumani K, Hwang DS, Desai BM, Zhang D, Dayes N, Green DR, Weiner DB. HIV-1 Vpr induces apoptosis through caspase 9 in T cells and peripheral blood mononuclear cells. J Biol Chem. 2002;277:37820–31.
30. Laird MD, Shields JS, Sukumari-Ramesh S, Kimbler DE, Fessler RD, Shakir B, Youssef P, Yanasak N, Vender JR, Dhandapani KM. High mobility group box protein-1 promotes cerebral edema after traumatic brain injury via activation of toll-like receptor 4. Glia. 2014;62:26–38.
31. Muthumani K, Lankaraman KM, Laddy DJ, Sundaram SG, Chung CW, Sako E, Wu L, Khan A, Sardesai N, Kim JJ, et al. Immunogenicity of novel consensus-based DNA vaccines against Chikungunya virus. Vaccine. 2008;26:5128–34.
32. Shim JH, Xiao C, Paschal AE, Bailey ST, Rao P, Hayden MS, Lee KY, Bussey C, Steckel M, Tanaka N, et al. TAK1, but not TAB1 or TAB2, plays an essential role in multiple signaling pathways in vivo. Genes Dev. 2005;19:2668–81.
33. Hayden MS, Ghosh S. Signaling to NF-kappaB. Genes Dev. 2004;18:2195–224.
34. Oeckinghaus A, Hayden MS, Ghosh S. Crosstalk in NF-kappaB signaling pathways. Nat Immunol. 2011;12:695–708.
35. Hayden MS, West AP, Ghosh S. SnapShot: NF-kappaB signaling pathways. Cell. 2006;127:1286–7.
36. Scheeren FA, Kuo AH, van Weele LJ, Cai S, Glykofridis I, Sikandar SS, Zabala M, Qian D, Lam JS, Johnston D, et al. A cell-intrinsic role for TLR2–MYD88 in intestinal and breast epithelia and oncogenesis. Nat Cell Biol. 2014;16:1238–48.
37. Gonzalez-Navajas JM, Lee J, David M, Raz E. Immunomodulatory functions of type I interferons. Nat Rev Immunol. 2012;12:125–35.
38. Moser M, Murphy KM. Dendritic cell regulation of TH1-TH2 development. Nat Immunol. 2000;1:199–205.
39. Zhou L, Ivanov II, Spolski R, Min R, Shenderov K, Egawa T, Levy DE, Leonard WJ, Littman DR. IL-6 programs T(H)-17 cell differentiation by promoting sequential engagement of the IL-21 and IL-23 pathways. Nat Immunol. 2007;8:967–74.
40. Aghbash PS, Hemmat N, Nahand JS, Shamekh A, Memar MY, Babaei A, Baghi HB. The role of Th17 cells in viral infections. Int Immunopharmacol. 2021;91: 107331.
41. Martinez NE, Sato F, Kawai E, Omura S, Chervenak RP, Tsunoda I. Regulatory T cells and Th17 cells in viral infections: implications for multiple sclerosis and myocarditis. Future Virol. 2012;7:593–608.
42. Heinrichsdorff J, Luedde T, Perdiguero E, Nebreda AR, Pasparakis M. p38 alpha MAPK inhibits JNK activation and collaborates with IkappaB kinase 2 to prevent endotoxin-induced liver failure. EMBO Rep. 2008;9:1048–54.
43. Dambach DM. Potential adverse effects associated with inhibition of p38alpha/beta MAP kinases. Curr Top Med Chem. 2005;5:929–39.
44. Tao W, Mao X, Davide JP, Ng B, Cai M, Burke PA, Sachs AB, Sepp-Lorenzino L. Mechanistically probing lipid-siRNA nanoparticle-associated toxicities identifies Jak inhibitors effective in mitigating multifaceted toxic responses. Mol Ther. 2011;19:567–75.
45. Aoki CA, Borchers AT, Ridgway WM, Keen CL, Ansari AA, Gershwin ME. NOD mice and autoimmunity. Autoimmun Rev. 2005;4:373–9.
46. Atkinson MA, Maclaren NK. The pathogenesis of insulin-dependent diabetes mellitus. N Engl J Med. 1994;331:1428–36.
47. Drage M, Zaccone P, Phillips JM, Nicoletti F, Dawson J, Andrew Bradley J, Cooke A. Nondepleting anti-CD4 and soluble interleukin-1 receptor prevent autoimmune destruction of syngeneic islet grafts in diabetic NOD mice. Transplantation. 2002;74:611–9.
48. Nicoletti F, Di Marco R, Barcellini W, Magro G, Schorlemmer HU, Kurrle R, Lunetta M, Grasso S, Zaccone P, Meroni P. Protection from experimental autoimmune diabetes in the non-obese diabetic mouse with soluble interleukin-1 receptor. Eur J Immunol. 1994;24:1843–7.
49. Nicoletti F, Di Marco R, Zaccone P, Magro G, Di Mauro M, Grasso S, Meroni PL. Endogenous interleukin-12 only plays a key pathogenetic role in non-obese diabetic mouse diabetes during the very early stages of the disease. Immunology. 1999;97:367–70.
50. Trembleau S, Penna G, Gregori S, Gately MK, Adorini L. Deviation of pancreas-infiltrating cells to Th2 by interleukin-12 antagonist administration inhibits autoimmune diabetes. Eur J Immunol. 1997;27:2330–9.
51. Debray-Sachs M, Carnaud C, Boitard C, Cohen H, Gresser I, Bedossa P, Bach JF. Prevention of diabetes in NOD mice treated with antibody to murine IFN gamma. J Autoimmun. 1991;4:237–48.
52. Nicoletti F, Zaccone P, Di Marco R, Di Mauro M, Magro G, Grasso S, Mughini L, Meroni P, Garotta G. The effects of a nonimmunogenic form of murine soluble interferon-gamma receptor on the development of autoimmune diabetes in the NOD mouse. Endocrinology. 1996;137:5567–75.
53. Zaccone P, Phillips J, Conget I, Cooke A, Nicoletti F. IL-18 binding protein fusion construct delays the development of diabetes in adoptive transfer and cyclophosphamide-induced diabetes in NOD mouse. Clin Immunol. 2005;115:74–9.
54. Bradshaw EM, Raddassi K, Elyaman W, Orban T, Gottlieb PA, Kent SC, Hafler DA. Monocytes from patients with type 1 diabetes spontaneously secrete proinflammatory cytokines inducing Th17 cells. J Immunol. 2009;183:4432–9.
55. Arif S, Moore F, Marks K, Bouckenooghe T, Dayan CM, Planas R, Vives-Pi M, Powrie J, Tree T, Marchetti P, et al. Peripheral and islet interleukin-17 pathway activation characterizes human autoimmune diabetes and promotes cytokine-mediated beta-cell death. Diabetes. 2011;60:2112–9.

56. Fores JP, Crisostomo LG, Orii NM, Santos AS, Fukui RT, Matioli SR, de Moraes VD, Silva M. Th17 pathway in recent-onset autoimmune diabetes. Cell Immunol. 2018;324:8–13.
57. Gandhi M, Alwawi E, Gordon KB. Anti-p40 antibodies ustekinumab and briakinumab: blockade of interleukin-12 and interleukin-23 in the treatment of psoriasis. Semin Cutan Med Surg. 2010;29:48–52.

Publisher's Note